

# A new NMR method for directly monitoring and quantifying the dissolution kinetics of starch in DMSO

Anthony Dona,<sup>a,b</sup> Chun-Wai Wayne Yuen,<sup>a</sup> Jonathan Peate,<sup>a,b</sup> Robert G. Gilbert,<sup>b</sup> Patrice Castignolles<sup>a,b</sup> and Marianne Gaborieau<sup>a,b,\*</sup>

<sup>a</sup>Key Centre for Polymer Colloids, School of Chemistry F11, University of Sydney, NSW 2006, Australia

<sup>b</sup>CNAFS/SLCAFS, Hartley Teakle Building 83, The University of Queensland, St Lucia QLD 4072, Australia

Received 29 April 2007; received in revised form 30 July 2007; accepted 19 August 2007

Available online 24 August 2007

**Abstract**—The kinetics of dissolution of starch is needed for (i) understanding digestive processes; (ii) providing data that could correlate with higher levels of starch structure; (iii) improving techniques for starch characterization in solution. A novel method is presented here to directly monitor these dissolution kinetics by time-resolved <sup>1</sup>H solution-state nuclear magnetic resonance (NMR); studies were carried out in deuterated dimethyl sulfoxide (DMSO-*d*<sub>6</sub>). By assuming pseudo-first-order kinetics with respect to starch concentration, the data for various starch samples yield values of the apparent rate coefficients for the rate of appearance of completely dissolved anhydroglucose units, results which have not been obtained hitherto. The presence of a limited amount of water in DMSO had a drastic effect on dissolution kinetics (slowing it down at high temperatures), indicating multiple pathways for the dissolution mechanism. Dynamic light scattering (DLS) appears to be more limited than the NMR method to monitor the kinetics of dissolution. The newly developed NMR method can be extended to other solvents and polysaccharides.

© 2007 Elsevier Ltd. All rights reserved.

**Keywords:** Dissolution kinetics; Time-resolved <sup>1</sup>H nuclear magnetic resonance (NMR); Dynamic light scattering (DLS); Starch; Anhydrous DMSO

## 1. Introduction

Understanding the mechanism and structural parameters controlling the rate at which starch dissolves has a number of applications. The first is in human and animal nutrition, for example, as measured by glycemic index (GI)<sup>1</sup> and resistant starch.<sup>2</sup> Second, the rate of dissolution of a particular starch sample is an intrinsic physical property, which might correlate with, and provide information on, structural characteristics such as the arrangement of chains in the semi-crystalline starch granule. Third, it might be helpful in fully dissolving starch for further characterization.

Investigating the molecular structure and some physical properties of starch requires dissolving starch molecules without degrading them. Many chromatography techniques have been applied to debranched starch (cap-

illary electrophoresis,<sup>3</sup> ionic chromatography<sup>4</sup>) or native starch (size exclusion chromatography, SEC or GPC,<sup>5–8</sup> field-flow fractionation<sup>9</sup>), while light scattering<sup>10</sup> and viscometry<sup>11</sup> give useful information about the size of starch molecules. Starch–water ‘solutions’ used for analysis are usually suspensions, as starch is only partially soluble in water.<sup>12–15</sup> Furthermore, aqueous solvents, which solubilize starch, such as sodium hydroxide solutions, may also degrade it.<sup>16</sup> These starch solutions precipitate spontaneously and in a non-repeatable fashion (‘retrogradation’).<sup>13,17</sup> These factors make solubility and gelatinization of starch in different solvents a widely researched topic.<sup>17–20</sup> While directly investigating biological processes requires that the solvent be water-based, the problems with dissolution in aqueous systems limit their use in investigating starch structure. The most widely used organic solvent for starch is dimethyl sulfoxide (DMSO).<sup>21</sup> However, dissolution of starch in different solvents is known to occur via different pathways.<sup>20,22</sup>

\* Corresponding author. Fax: +61 3365 1188; e-mail: [m.gaborieau@uq.edu.au](mailto:m.gaborieau@uq.edu.au)

Starch dissolution has been previously studied using techniques such as polarized optical microscopy (which monitors the loss of crystallinity)<sup>20</sup> or differential scanning calorimetry.<sup>23</sup> The inverse process, retrogradation, has been monitored by rheology, X-ray diffraction, thermal analysis, and nuclear magnetic resonance (NMR).<sup>24,25</sup> The NMR techniques used hitherto all indirectly monitor retrogradation via mobility changes within the sample.

The present paper develops a new tool to study the kinetics of starch dissolution, in situ time-resolved nuclear magnetic resonance (NMR),<sup>26</sup> consisting of recording sequential  $^1\text{H}$  spectra of a sample in the spectrometer. This technique has been used in the past to directly monitor the kinetics of reaction (polymerization,<sup>27,28</sup> in vivo metabolism<sup>29</sup>) and of phase change (dissolution,<sup>30</sup> protein folding,<sup>31</sup> crystallization<sup>32</sup>). The advantage of this technique compared to those previously used to study starch dissolution kinetics is that  $^1\text{H}$  NMR quantitatively detects the dissolved species, and only the dissolved species, and thus the signal intensity will increase proportionally to the number of anhydroglucose units entering solution. The present paper thus gives the first method able to provide reliable rates of dissolution for starch in terms of appearance of completely dissolved anhydroglucose units. To exemplify the new method, we give some dissolution data for starch in anhydrous and wet DMSO. Data so obtained are not in themselves sufficient to reveal the mechanism, but along with other information from, for example, polarized optical microscopy could in the future be used to check mechanistic hypotheses and provide a convenient means of comparing different samples. More complete understanding of the complex dissolution mechanism of starch is reserved for future work. Dynamic light scattering (DLS)<sup>33</sup> is also evaluated as an alternative technique to directly follow starch dissolution in DMSO.

## 2. Results and discussion

### 2.1. Principle of the in situ time-resolved $^1\text{H}$ solution-state NMR method

Sequential  $^1\text{H}$  NMR experiments are recorded on a sample left in the spectrometer, monitoring the increase in the integral under the starch signals. This integral is directly proportional to the amount of starch dissolved when spectra are recorded with a sufficiently long relaxation delay. Figure 1(top) displays an example of consecutive spectra obtained on dissolving a Sigma starch sample in anhydrous  $\text{DMSO}-d_6$  at 60 °C. It demonstrates the increase in intensity of the starch lines between 2.7 and 5.5 ppm,<sup>34,35</sup> while the integral under the residual DMSO line at 2.5 ppm remains constant.

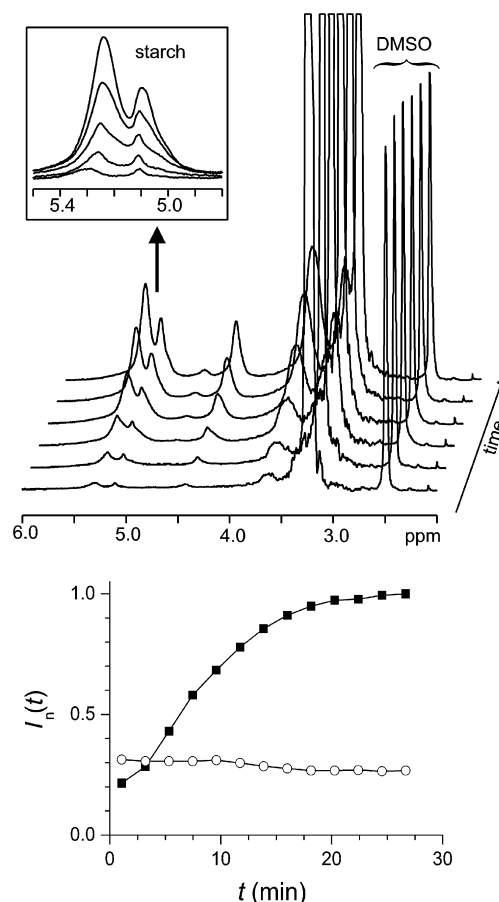


**Figure 1.** (Top) Sequential  $^1\text{H}$  NMR spectra recorded during the dissolution of Sigma starch in anhydrous  $\text{DMSO}-d_6$  at 60 °C. Lines between 2.7 and 5.5 ppm correspond to starch signals<sup>34,35</sup> and the line at 2.5 ppm is the signal from residual DMSO. Inset: overlaid spectral lines between 5 and 5.3 ppm. (Bottom) Time evolution of  $^1\text{H}$  NMR integrated signals for this dissolution experiment (full squares: starch, hollow circles: residual DMSO) obtained by time-resolved NMR.

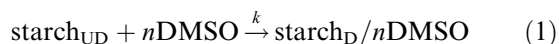
The signals were integrated on each spectrum between 4.2 and 7.0 ppm for starch, and between 2.1 and 2.8 ppm for residual DMSO. The time considered for each spectrum is the average of the times at the beginning and at the end of the spectrum recording. The signal integrals were normalized to give the quantity  $I_n(t)$  at each time by dividing these integrals by the final signal integral for starch. Figure 1(bottom) displays the growth of the starch signals compared to the constant DMSO signal integral. All samples exhibited a similar increase in starch signals and a constant residual DMSO signal, on different time scales.

The repeatability of the technique was checked on Sigma starch in anhydrous  $\text{DMSO}-d_6$  at 60 °C (Fig. S9).

### 2.2. Apparent dissolution rate coefficients

The kinetics of dissolution of a simple polymer into solution is complex.<sup>36,37</sup> Starch is a semi-crystalline

hydrogen-bonded polymer, introducing further complexity to the dissolution process.<sup>38</sup> As a starting point for kinetic analysis, it was assumed that the rate is a pseudo-first order in the amount of undissolved starch. This is emphatically not a model for the kinetics, but it allows us to extract values of apparent dissolution rates in order to compare samples. The physical change is then expressed in Eq. 1:



where starch<sub>UD</sub> and starch<sub>D</sub>/nDMSO are undissolved and dissolved starch, respectively,  $n$  is the number of DMSO- $d_6$  molecules necessary to dissolve one molecule of starch, and  $k$  is the rate coefficient for the physical change. The resulting rate equation is then given by Eq. 2:

$$\frac{d[\text{starch}_{\text{D}}/n\text{DMSO}]}{dt} = k[\text{starch}_{\text{UD}}][\text{DMSO}]^n \quad (2)$$

where  $t$  is the time. As  $[\text{DMSO}]^n$  is constant we can define  $k[\text{DMSO}]^n$  as  $k_{\text{app}}$ , the apparent first-order rate coefficient of dissolution. To test the validity of the pseudo-first-order assumption, the normalized experimental data were plotted versus time as the function  $f(t)$  of Eq. 3:

$$f(t) = \ln\left(\frac{1}{1 - I_n(t)}\right) \quad (3)$$

Straight lines were obtained for this plot (Figs. 2 and S1–S6), suggesting that the admittedly simplistic assumption of first-order kinetics with respect to starch concentration is adequate. Furthermore, a plot of  $(1 - I_n(t))^{-1}$  versus time (which would be linear if second-order kinetics were applicable), shows distinct curvature (Fig. 2). The apparent rate coefficient  $k_{\text{app}}$  was measured as the slope of  $f(t)$  versus time. The technique enables us to quantitatively study the kinetics of dissolution of starch in different solvents and at different temperatures.

### 2.3. Effect of water and temperature

The dissolution of starch was faster in anhydrous DMSO- $d_6$  than in standard wet DMSO- $d_6$  (Fig. 3), especially at higher temperatures, as shown for 80 °C. This suggests different dissolution pathways. Using polarized optical microscopy (POM),<sup>20</sup> Mukerjea et al. proposed that starch dissolution occurs through the peeling of the granule in anhydrous DMSO; gel layers can be formed around the ungelatinized portion of the granules impeding dissolution. In binary DMSO–water mixtures, starch granules swell and the semi-crystalline characteristic of the granule is lost ('gelatinization').<sup>22</sup> With increasing swelling, the granules will burst, releasing starch into the solution. The present results, obtained by directly monitoring dissolution with NMR, indicate

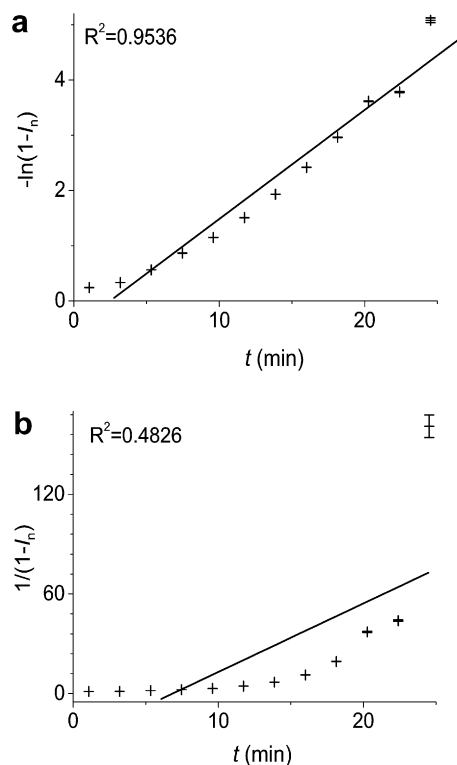


**Figure 2.** Experimental NMR data for Sigma starch dissolution in anhydrous DMSO- $d_6$  at 60 °C plotted to obtain a linear fit if the data follow (a) a first-order kinetics and (b) a second-order kinetics (crosses: experimental NMR data, solid lines: linear fits). The error bars are calculated as detailed in [Supplementary data](#), but not taken into account for the linear fits.

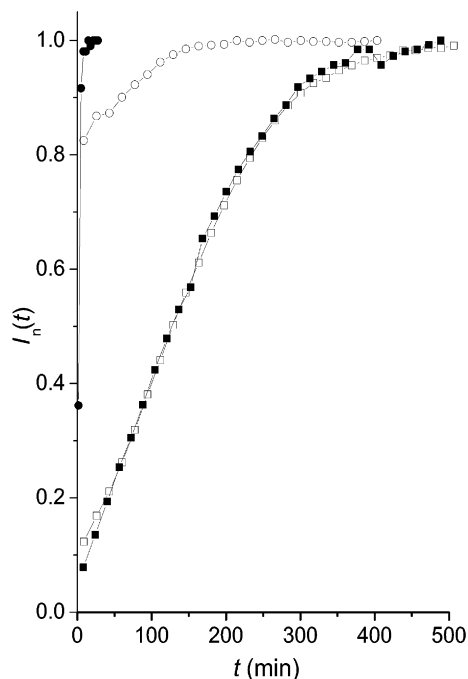


**Figure 3.** The dissolution curves of starch in anhydrous DMSO- $d_6$  (full symbols) and wet DMSO- $d_6$  (hollow symbols) at 37 °C (squares) and 80 °C (circles) obtained by time-resolved NMR.

that the rate of dissolution is slowed as the water content of the solvent increases (Fig. 3). On the other hand, crystallinity of starch disappears faster in a DMSO–water mixture of higher water content, as observed with polarized optical microscopy.<sup>20</sup> This apparent contradiction originates in the fact that granule swelling and loss of crystallinity are only one step in a multi-step dissolution process. Comparison of results obtained by the complementary polarized optical microscopy and NMR techniques suggests that although swelling by water is faster, actual starch dissolution through the peeling of the granule is faster in anhydrous solvent, when the granule is not swollen.

Anhydrous DMSO- $d_6$  provides faster starch dissolution with increasing temperatures (Figs. 3 and S7). The apparent rate coefficients for the dissolution of Sigma starch in anhydrous DMSO- $d_6$  were fitted with the Arrhenius equation, yielding an apparent activation energy of 85 kJ mol<sup>-1</sup> (Figs. 4 and S8). This large value suggests that the peeling of starch from the granule is opposed by strong intermolecular forces. However, it is noted that the temperature range of this study is much too low to conclude if the process actually follows an Arrhenius behavior.

Apparent dissolution rate coefficients were measured for three other rice starches in anhydrous DMSO- $d_6$  at several temperatures (Fig. 4 and Table S1); those starches exhibited a dissolution behavior very similar

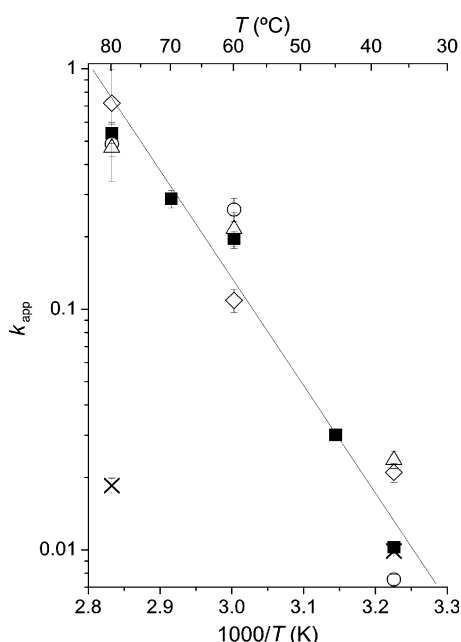


**Figure 4.** Temperature dependence of the apparent dissolution rate coefficient for rice starch varieties in anhydrous DMSO- $d_6$ , from 37 °C to 80 °C (squares: Sigma starch, circles: Doongara starch, triangles: Illabong starch, diamonds: Langi starch). The solid line is the Arrhenius fit for Sigma starch, weighted by inverse relative error (see Supplementary data). Dissolution behavior of Sigma starch in wet DMSO- $d_6$  is indicated by crosses.

to that of Sigma starch. These starches have significantly different glycemic indices,<sup>39</sup> and thus the kinetics of dissolution in DMSO is not directly related to digestibility. This can be rationalized considering that the glycemic index is linked to digestion in aqueous medium, while DMSO is an organic solvent, in which a different pathway is observed for starch dissolution. Chromatography techniques may bring more valuable information about digestibility, and DMSO may be a valuable solvent for this since the four starch samples studied in this work all exhibit comparable kinetics of dissolution in DMSO.

#### 2.4. Dissolution followed by dynamic light scattering

DLS is sensitive to both dissolved starch chains and aggregates. DLS is thus in principle a more powerful technique to follow dissolution kinetics than NMR, which is sensitive only to the dissolved starch chains. DLS provides some limited information on the distribution of sizes of the species present in the solution, via the detection of their motion; the process of inversion of DLS data to a size distribution is, however, an ill-conditioned problem and cannot give a unique answer. Moreover, DLS registers all types of local motions and translational diffusion due to thermal fluctuations of a system in thermal equilibrium. To probe starch size in solution, the scattering by the whole particle or macromolecule must be detected by DLS: therefore the measurements should be made in the limit of small values of the scattering vector  $q$ . One criterion is that  $qR_g \ll 1$ ,<sup>33</sup> where  $R_g$  is the radius of gyration of starch molecules; a later suggestion was that the translational diffusion of amylopectin is probed when  $qR_g \leq 2$ .<sup>40</sup>

In the present study, the effect of scattering angle (smaller angle resulting in smaller  $q$ ) on the effective diameter measured by DLS for a fully dissolved Sigma starch sample (80 °C, 1% w/v in anhydrous DMSO) was investigated (Fig. 5). Below 40°, the background noise is increased resulting in scattered values. At 50° and above, both local motions and translational diffusion may be probed, resulting in the measurement of a lower average size (Fig. S10). Thus, for the system used here, the optimal angle for reliable DLS measurement of Sigma starch is 40°. It should be noted that this study of the angular dependence of effective diameter measured by DLS depends on the value of  $R_g$  and thus does not apply to all starch samples.

DLS was tested as a technique to monitor the kinetics of dissolution by following either the decrease of the size of the aggregate or the disappearance of their peak (Tables S5–S7). During a DLS measurement, shear must be interrupted for 5–10 min, inducing a perturbation that is not encountered in the NMR experiment. Furthermore, a starch chain typically has a radius of ca 300 nm.<sup>41</sup> Using the size distributions, it is difficult to discriminate between aggregates and fully dissolved

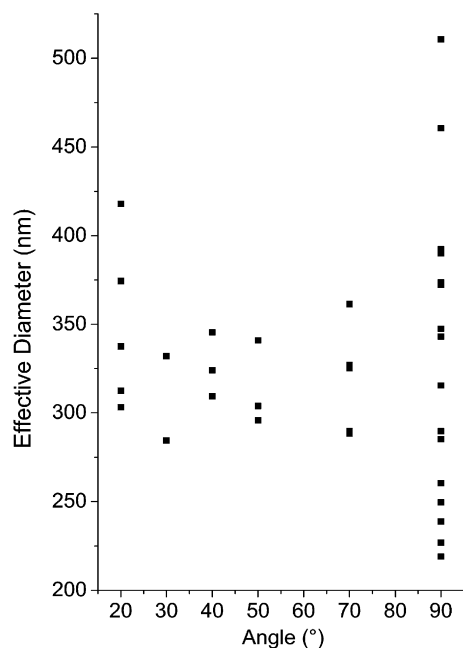


**Figure 5.** Change in effective diameter measured by DLS as a function of angle for Sigma starch in anhydrous DMSO at 80 °C.

starch chains. The dissolution was followed at 80 °C in anhydrous DMSO at an angle of 40°; repeating the experiment four times only indicated that aggregates might have disappeared after 30 min to 1 h, which is consistent with the NMR measurements. Thus, even limiting the number of measurements, the DLS results are far more difficult to interpret than the NMR ones. Note that this issue may be partially explained by the low refractive index increment  $dn/dc$  of starch in DMSO ( $<0.07$ )<sup>17</sup> and DLS may be a more favorable technique to monitor the dissolution of another polymer in another solvent.

### 3. Conclusions

The newly developed in situ time-resolved <sup>1</sup>H NMR technique is the first quantitative method to directly follow dissolution kinetics. It is applicable on timescales from 10 min to several hours. It has considerable potential to extend to other solvent and polysaccharide systems. While DLS is in principle more powerful, in practice it is not sufficiently accurate to follow the kinetics of dissolution.

The polarized optical microscopy method used in the literature is reliable, but follows the disappearance of crystallinity,<sup>20</sup> which is only one of the multi-step dissolution processes. The NMR results for the dissolution in DMSO at different water levels show that there are other significant steps in the dissolution process than the loss of crystallinity. Polarized optical microscopy is thus complementary to the time-resolved <sup>1</sup>H NMR

method for gaining understanding of the complex process of the dissolution of starch in various solvents.

The data for dissolution in DMSO-*d*<sub>6</sub> of a range of purified starch samples (Sigma starch and several rice starches) can be fitted as first order in concentration of undissolved starch. While this certainly does not imply that the mechanism is a simple first-order process, this result is a convenient one for quantitatively comparing data from different starch samples. The apparent activation energy is ca 85 kJ mol<sup>-1</sup>; this high value may indicate that strong intermolecular forces play a role in the dissolution process. While the present data are not in themselves sufficient to reveal the mechanism, along with other information, they can be used to check mechanistic hypotheses.

The time-resolved NMR method presented here can potentially be extended to any solvent and polymer systems to quantify dissolution kinetics.

## 4. Experimental

### 4.1. Materials

Rice starch was obtained from Sigma (S-7260) or from Rice Growers Co-operative (Langi, Illabong, and Doongara), Tricine (T-377) from Aldrich and protease (P-5147) from Sigma. DMSO-*d*<sub>6</sub> (99.9%) and deuterium oxide D<sub>2</sub>O (99.9%) were from Cambridge Isotope Laboratories Inc., and DMSO (99.5%) from Sigma (D-5879). Note that DMSO is hygroscopic. Anhydrous DMSO and anhydrous DMSO-*d*<sub>6</sub> were dried with excess 4 Å molecular sieves and filtered through a hydrophilic PTFE 0.2 µm Millipore filter; they were stored in a desiccator with desiccant in a bottle wrapped in Parafilm; the absence of water was checked using solution IR (by the absence of any absorption around 3000 cm<sup>-1</sup>). Undried DMSO is referred to as wet DMSO in the text.

### 4.2. Extraction of starch from rice varieties

Starch was extracted<sup>42</sup> from three rice varieties: Langi, Illabong, and Doongara. The rice (100 g) was milled (Retsch S100 centrifugal ball mill) with 3 × 30 mm and 4 × 20 mm steel ball bearings (2 h, 300 rpm), then with 2 × 20 mm and 12 × 10 mm steel ball bearings (2 h, 300 rpm) to pass through a 0.5 mm sieve. If the rice grains did not break in the ball mill, the sample was initially ground with mortar and pestle. To remove proteins, a tricine buffer solution (250 mM, 75 mL, pH 7.5) containing protease (0.9 U mL<sup>-1</sup>) was added to the resulting flour (15 g) and incubated (37 °C, 20 min). The sample was then centrifuged (10,500 g, 10 min) and the supernatant discarded while the precipitate was refluxed in a Soxhlet extractor (90 °C, 24 h) with



methanol (100 mL). The resulting suspension was filtered through a 0.45 µm cellulose acetate filter and the solid starch washed with ethanol then diethyl ether before drying in vacuum (16 h, 50 °C).

#### 4.3. Time-resolved $^1\text{H}$ solution-state NMR

$^1\text{H}$  NMR was performed on a Bruker Avance spectrometer at a  $^1\text{H}$  Larmor frequency of 300.13 Hz.  $^1\text{H}$  spectra of 1% (w/v) starch samples in (wet) DMSO- $d_6$  or anhydrous DMSO- $d_6$  were obtained between 37 °C and 80 °C in 5 mm NMR tubes spinning at 20 Hz (1200 rpm). The chemical shift scale was calibrated using the residual DMSO signal (2.49 ppm). A sample, which had dissolved to completeness, was used to lock, shim and optimize parameters: the 90° pulse length to a value between 6 and 8 µs and the sum of the acquisition time (AQ) and relaxation delay ( $d_1$ ) to a value between 8 and 30 s (for quantitative analysis, it was ensured that the integral of starch signals was unchanged for a five- or tenfold increase in AQ +  $d_1$  delay). Immediately after this, a freshly prepared sample of the same nature (starch type, concentration, solvent) had 15–50 experiments recorded every 2–15 min (24–128 scans). The data were processed using x-winnmr software. The parameters used are given in [Supplementary data \(Tables S2 and S3\)](#).

#### 4.4. DLS

Dynamic light scattering (DLS) was performed on a photon correlation spectrophotometer (PCS, Brookhaven) comprising a BI-200SM Version 2 goniometer with a 633 nm 35 mW HeNe laser, a BI-APD Avalanche Photodiode Detector, and a PC1 BI-9000AT EN correlator. The sample temperature was controlled by heating decalin in the void volume. The intensity measured in DLS varies as the 6th power of the radius; it is thus extremely sensitive to large particles such as dust, which might be confused with aggregates. Minimal dust contamination was assured by filtering the solvent through three hydrophilic PTFE 0.2 µm Millipore filters and rinsing vials three times with filtered solvent. Obtaining the same size for samples prepared the same way ensured the absence of dust. All measurements were repeated at least twice, and some were repeated by another operator on another day to check the robustness of the procedure. Viscosity and refractive index values for anhydrous DMSO at 80 °C,  $\eta = 0.84$  cP (1 cP = 1 mPa s), and  $n = 1.4485$  were interpolated from literature values<sup>43–45</sup> ([Fig. S11](#)). Only anhydrous DMSO was used, since the water content of wet DMSO was not known precisely and it modifies the viscosity. Between measurements the vial was shaken in a thermomixer at 300 rpm (minimal possible shaking), as magnetic stirring may provide enough shear degrade starch chains.<sup>46</sup> The

glass vials were sealed by rubber septa, which may lead to contamination of the solution either instantaneously when a direct contact with the DMSO occurs or after two days with DMSO at 80 °C even if no direct contact occurred. Rubber septa have been reported in the literature to pollute DMSO with fluorescent species;<sup>17</sup> this was checked by DLS measurement of pure DMSO in a glass vial sealed by a rubber septum ([Supplementary data, Table S4 and Fig. S12](#)); all potentially contaminated samples were discarded. Only experimental runs with less than 500 kilocounts per second in average were used. Any features in a size distribution produced by PCS software must be tested for artifacts by varying the basic assumptions as to the form of the distribution (e.g., CONTIN vs NLLS<sup>47,48</sup>) and numerical parameters in the inversion such as integration range. Only results for which both CONTIN and NLLS deconvolution routines gave qualitatively similar results in terms of number and maxima of size populations in the intensity distribution were considered.

#### Acknowledgement

The authors thank Hank De Bruyn for help with the Brookhaven set-up and Astley Friend for some DLS measurements. The Key Centre for Polymer Colloids was established and supported by the Australian Research Council's Research Centres Program. We gratefully acknowledge funding from an Australian Research Council Discovery project.

#### Supplementary data

Supplementary data associated with this article (including [Figs. S1–S12](#) as well as [Tables S1–S7](#)) can be found, in the online version, at [doi:10.1016/j.carres.2007.08.010](https://doi.org/10.1016/j.carres.2007.08.010).

#### References

- Jenkins, D. J.; Wolever, T. M.; Taylor, R. H.; Barker, H.; Fielden, H.; Baldwin, J. M.; Bowling, A. C.; Newman, H. C.; Jenkins, A. L.; Goff, D. V. *Am. J. Clin. Nutr.* **1981**, *34*, 362–366.
- Bird, A. R.; Vuaran, M.; Brown, I.; Topping, D. L. *Br. J. Nutr.* **2007**, *97*, 134–144.
- O'Shea, M. G.; Samuel, M. S.; Konik, C. M.; Morell, M. K. *Carbohydr. Res.* **1998**, *307*, 1–12.
- Hanashiro, I.; Abe, J.; Hizukuri, S. *Carbohydr. Res.* **1996**, *283*, 151–159.
- Bello-Perez, L. A.; Roger, P.; Baud, B.; Colonna, P. *J. Cereal Sci.* **1998**, *27*, 267–278.
- Chen, Y. F.; Fringant, C.; Rinaudo, M. *Carbohydr. Polym.* **1997**, *33*, 73–78.
- Hizukuri, S.; Takagi, T. *Carbohydr. Res.* **1984**, *134*, 1–10.

8. Striegel, A. M.; Timpa, J. D. *Carbohydr. Res.* **1995**, *267*, 271–290.
9. Roger, P.; Baud, B.; Colonna, P. *J. Chromatogr. A* **2001**, *917*, 179–185.
10. Galinsky, G.; Burchard, W. *Macromolecules* **1995**, *28*, 2363–2370.
11. Everett, W. W.; Foster, J. F. *J. Am. Chem. Soc.* **1959**, *81*, 3464–3469.
12. Ramesh, M.; Ali, S. Z.; Bhattacharya, K. R. *Starch/Staerke* **1999**, *51*, 308–310.
13. Roger, P.; Tran, V.; Leseq, J.; Colonna, P. *J. Cereal Sci.* **1996**, *24*, 247–262.
14. Ward, R. M.; Gao, Q.; de Bruyn, H.; Lamb, D. J.; Gilbert, R. G.; Fitzgerald, M. A. *Biomacromolecules* **2006**, *7*, 866.
15. Roger, P.; Bello-Perez, L. A.; Colonna, P. *Polymer* **1999**, *40*, 6897–6909.
16. BeMiller, J. N. Alkaline degradation of starch. In *Starch: Chemistry and Technology*; Academic Press: New York, 1965; pp 521–532.
17. Everett, W. W.; Foster, J. F. *J. Am. Chem. Soc.* **1959**, *81*, 3459–3464.
18. Killion, P. J.; Foster, J. F. *J. Polym. Sci.* **1960**, *46*, 65–73.
19. Leach, H. W.; Schoch, T. J. *Cereal Chem.* **1962**, *39*, 318–327.
20. Mukerjea, R.; Mukerjea, R.; Robyt, J. F. *Carbohydr. Res.* **2006**, *341*, 757–765.
21. Hizukuri, S. *Food Sci. Technol.* **1996**, *74*, 347–429.
22. Tester, R. F.; Somerville, M. D. *Food Hydrocoll.* **2002**, *17*, 41–54.
23. Yeh, A. I.; Li, J. Y. *Starch/Staerke* **1996**, *48*, 17–21.
24. Abd Karim, A.; Norziah, M. H.; Seow, C. C. *Food Chem.* **2000**, *71*, 9–36.
25. Lewen, K. S.; Paeschke, T.; Reid, J.; Molitor, P.; Schmidt, S. J. *J. Agric. Food Chem.* **2003**, *51*, 2348–2358.
26. Claridge, T. D. W. *High-Resolution NMR Techniques in Organic Chemistry*; Elsevier: Amsterdam, 1999.
27. Haddleton, D. M.; Perrier, S.; Bon, S. A. F. *Macromolecules* **2000**, *33*, 8246–8251.
28. Lienkamp, K.; Schnell, I.; Groehn, F.; Wegner, G. *Macromol. Chem. Phys.* **2006**, *207*, 2066–2073.
29. Mulquiney, P. J.; Bubb, W. A.; Kuchel, P. W. *Biochem. J.* **1999**, *342*, 567–580.
30. Devotta, I.; Badiger, M. V.; Rajamohanam, P. R.; Ganapathy, S.; Mashelkar, R. A. *Chem. Eng. Sci.* **1995**, *50*, 2557–2569.
31. Cemazar, M.; Zahariev, S.; Pongor, S.; Hore, P. J. *J. Biol. Chem.* **2004**, *279*, 16697–16705.
32. Yushmanov, P. V.; Furo, I.; Stilbs, P. *Colloid Surf. A-Physicochem. Eng. Asp.* **2006**, *291*, 59–62.
33. Galinsky, G.; Burchard, W. *Macromolecules* **1997**, *30*, 6966–6973.
34. Andersson, L.; Andersson, R.; Andersson, R. E.; Rydberg, U.; Larsson, H.; Aman, P. *Carbohydr. Polym.* **2002**, *50*, 249–257.
35. Nilsson, G. S.; Bergquist, K. E.; Nilsson, U.; Gorton, L. *Starch/Staerke* **1996**, *48*, 352–357.
36. Narasimhan, B.; Peppas, N. A. *Adv. Polym. Sci.* **1997**, *128*, 157–207.
37. Miller-Chou, B. A.; Koenig, J. L. *Prog. Polym. Sci.* **2003**, *28*, 1223–1270.
38. Devotta, I.; Mashelkar, R. A. *Chem. Eng. Sci.* **1996**, *51*, 3881–3885.
39. Foster-Powell, K.; Holt, S. H. A.; Brand-Miller, J. C. *Am. J. Clin. Nutr.* **2002**, *76*, 5–56.
40. Yang, C.; Meng, B.; Chen, M.; Liu, X.; Hua, Y.; Ni, Z. *Carbohydr. Polym.* **2006**, *64*, 190–196.
41. Zhong, F.; Yokoyama, W.; Wang, Q.; Shoemaker, C. F. *J. Agric. Food Chem.* **2006**, *54*, 2320–2326.
42. Chiou, H.; Martin, M.; Fitzgerald, M. *Starch/Staerke* **2002**, *54*, 415–420.
43. Bicknell, R. T. M.; Davies, D. B.; Lawrence, K. G. *J. Chem. Soc., Faraday Trans. 1* **1982**, *78*, 1595–1601.
44. Saleh, M. A.; Ahmed, O.; Ahmed, M. S. *J. Mol. Liq.* **2004**, *115*, 41–47.
45. Kapadi, U. R.; Chavan, S. K.; Yemul, O. S. *J. Chem. Eng. Data* **1997**, *42*, 548–550.
46. Han, J. A.; Lim, S. T. *Carbohydr. Polym.* **2004**, *55*, 265–272.
47. Cao, X.; Sessa, D. J.; Wolf, W. J.; Willett, J. L. *Macromolecules* **2000**, *33*, 3314–3323.
48. Bello-Perez, L. A.; Roger, P.; Colonna, P.; Paredes-Lopez, O. *Carbohydr. Polym.* **1998**, *37*, 383–394.